CrystEngComm

COMMUNICATION

Rapid augmentation of vertically aligned MoO₃ nanorods *via* microwave irradiation†

Kaushalendra K. Singh, Vivek Ramakrishnan, [iD]
Ramya Prabhu B. and Neena S. John [iD] *

We have demonstrated a simple, low cost and swift method to prepare vertically aligned hexagonal MoO₃ nanorods on substrates using microwave irradiation. Most interestingly, the hexagonal rods can be converted to layered α-MoO₃ keeping the vertical alignment intact.

In the present scenario, materials with specific length scales on the order of nanometers attract immense interest because of their potential application in both the scientific and the industrial world. Nanomaterials with a specific structure, order and orientation are the subject of research and product development because they could be potentially applied to macroscopic devices owing to their catalytic, magnetic, optical, semiconductor, or other superior properties.[1]

Numerous approaches have been reported for the preparation of these micro–nano structures, *viz.*, hydrothermal, physical and chemical vapour deposition, electron and laser beam induced deposition, microwave (MW) irradiation, *etc.*[2,3] Even though the hydrothermal method is one of the most extensively employed solution-based chemical methods for the synthesis of a host of nanostructured materials, the reaction times are longer. MW assisted synthesis of nanostructured systems has been extensively employed in recent times[4–6] following the pioneering work on organic synthesis.[7,8] The main advantage of MW assisted synthesis is the reduced time consumption from several hours to several minutes or even seconds![9] In addition to the faster reaction time, it has various advantages such as eco-friendliness, cost-effectiveness, rapid heating, increased reaction kinetics and higher product yields amongst many others.

Transition metal oxides are well known for their catalytic activity and semiconducting nature.[10,11] MoO₃ is a promising functional material with a direct bandgap of 2.8–3.6 eV.[12]

MoO₃ based systems have found diverse applications in catalysis, field emitting diodes, sensors, batteries, fuel cells, photo and electro-catalysts, and photo-chromic and electro-chromic devices owing to their structure, size and shape dependent material properties.[13–16] Crystalline MoO₃ is reported to have three polymorphs: orthorhombic (α-MoO₃ – thermodynamically stable), monoclinic (β-MoO₃ – metastable) and hexagonal (h-MoO₃ – metastable) phases.[13] Orthorhombic α-MoO₃ consists of stacked bilayer sheets of MoO₆ octahedra held by van der Waals forces. It has a highly anisotropic layered structure along the [010] direction. On the other hand, hexagonal h-MoO₃ possesses large one-dimensional (1D) tunnels along the [001] direction, having zig-zag chains of [MoO₆] octahedra as the building blocks interlinked through the *cis*-position. Even though α-MoO₃ is the thermodynamically stable form, the tunnel structure of h-MoO₃ gives an added effect for electron–hole separation under light irradiation. This factor enhances the catalytic activity of h-MoO₃ compared with α-MoO₃.[12]

In this work, we have studied the synthesis and morphology of uniform, vertically aligned h-MoO₃ nanorods (NRs) on rigid substrates by MW irradiation using ammonium heptamolybdate (AHM) and concentrated nitric acid as the precursors. The vertical alignment of the nanorods results in structural anisotropy and is preferred for device fabrication as transport through oriented structures can be well understood. Charge transport through aligned metal oxide nanorods is more efficient due to less scattering and it also enables addressability of such arrays. This has been well documented in the case of vertically aligned nanostructures of ZnO and TiO₂, which are widely employed in photovoltaics and piezotronics.[17,18] In the present study, vertically oriented nanorods are obtained on seeded substrates within 90 s by MW irradiation. Although there are numerous reports on the preparation of h-MoO₃ NRs even *via* MW synthesis, this is the first report on the MW assisted vertically aligned growth of MoO₃ NRs to the best of our knowledge.[19–21]

The effect of MW power on the crystal structure and morphology of the NRs was initially studied in the solution

Centre for Nano and Soft Matter Sciences (CeNS), Jalahalli, Bengaluru – 560013, India. E-mail: jsneena@cens.res.in

phase, which facilitated the optimization of a suitable MW power for growing oriented NRs on rigid substrates. For the synthesis of NRs in the solution phase, 10 mL of 0.02 M aqueous solution of AHM was mixed with 5 mL of concentrated nitric acid and stirred well. This precursor solution mixture was transferred to a closed Teflon-lined vessel and was irradiated with MWs using a domestic MW oven. The white powder obtained from the reaction was washed well with deionized water and dried.

The morphologies of the as-synthesized h-MoO_3 NRs formed in solution at varying powers of 80, 160, 240, 320, 400, 480 and 560 W with an irradiation time of 300 s were examined by field emission scanning electron microscopy (FESEM) and are given in Fig. S1 (ESI†). At the low power of 80 W, the particles agglomerate, showing a spherical morphology. As the power is varied from 160–320 W, the hexagonal morphology becomes more defined and a mixture of isolated and flower-shaped NRs can be identified. It is also observed that the size of the structures increased with increasing irradiation power (Tables S1a and S2, ESI†). When the power is increased beyond 320 W, the same trend follows for the size of the NRs, however, defects start to appear in the form of broken, distorted and hollow hexagons. The NRs formed at 320 W showed the most defined hexagonal facets with almost no visible defects, and thus this power was chosen for growing oriented NRs. The formation of h-MoO_3 NRs was further confirmed by X-ray diffraction (XRD) (Fig. S2a, ESI†), Raman spectroscopy[22] (Fig. S2b, ESI†), and EDS analysis (Fig. S2c, ESI†). The XRD pattern shows diffraction peaks consistent with the standard hexagonal phase of MoO_3 (JCPDS card no. 21-0569). The effect of the power on the crystallinity of the NRs is shown in Fig. S3, ESI,† which compares the XRD patterns of the NRs obtained at 80, 320 and 560 W. An obvious trend can be observed with power; the diffraction pattern obtained at 80 W shows no distinct peaks, indicating that the synthesized spherical structures are amorphous. The crystalline character of the MoO_3 NRs is clearly improved at 320 W, where sharp diffraction peaks corresponding to the (100), (210), (300), (008), (218), (610) and (524) planes can be identified. With the increase in the irradiation power to 560 W, the intensities of the (100), (200) and (300) diffraction peaks increased further, suggesting the preferential growth of h-MoO_3 crystals along the (h00) direction.

The growth of h-MoO_3 NRs in solution was extended to rigid substrates such as SiO_2 and FTO. Synthesis parameters such as irradiation time and precursor concentration were then systematically varied and their corresponding effect on the vertically aligned NRs was studied in detail. To accomplish the aligned growth of NRs, a seed layer was coated on the substrates before MW irradiation by placing them in an inclined manner in the beaker containing the precursor solution and was heated at 80 °C for 30 min. In the final step, these seeded substrates were placed, in a similar manner to that mentioned above, inside the closed Teflon-lined vessel containing the precursor solution and irradiated at the selected MW power. Fig. 1(a)–(d) show the morphology of the
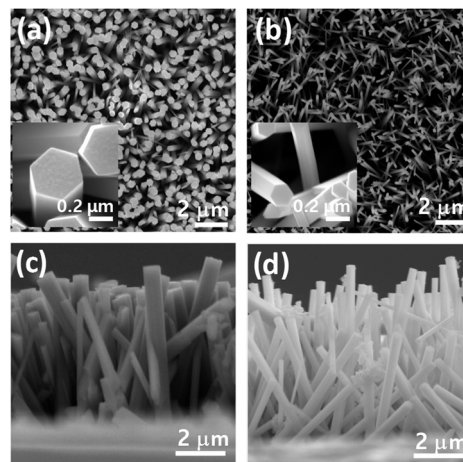

Fig. 1 FESEM images showing the top and side views of vertically grown h-MoO_3 NRs on different substrates: (a) and (c) FTO and (b) and (d) SiO_2, and zoom-in views (insets) obtained at a MW irradiation power of 320 W for 300 s in 0.02 M AHM.

h-MoO_3 NRs grown on FTO and SiO_2 substrates under optimized conditions. For the same synthesis conditions, the size of the NRs grown on SiO_2 and FTO was different. The average diameter of the rods formed on FTO (420 nm) is larger than that on SiO_2 (170 nm). The average aspect ratio (length/width, AR) of the NRs grown on SiO_2 is 36.9 while that of the NRs grown on FTO is 13.9 (Table S1b, ESI†). Calculations show that average angle of MoO_3 NRs on FTO and SiO_2 are 83° and 67°, respectively (Fig. S4, ESI†). Interestingly, seeding is found to have a significant influence on the morphology of MoO_3 NRs as evident from Fig. 1 and S5 (ESI†). On the unseeded substrates, flower-shaped hexagonal NRs were observed with no alignment in any particular direction, and the substrate–NR adhesion was also poor. However, with seeding, the grown aligned NRs were highly adherent, uniform and oriented vertically to the substrate. The seeding step is important for the formation of the NRs as it introduces heterogeneous nucleation sites which lead to the oriented growth of the structures.[23] The effect of MW irradiation time on the growth of the NRs was further studied. Fig. 2 shows the top view and cross sectional images of the vertically aligned NRs with corresponding MW irradiation times of 90 (Fig. 2a and c) and 180 s (Fig. 2b and d), which can be compared with the NRs formed at 300 s (Fig. 1a and c). The AR of the NRs was observed to increase from 10.6 to 13.9 as the MW irradiation time was increased from 90 to 300 s, which emphasizes the tunability of the NR size by controlling the synthesis time (Table 1).

Vertically aligned NRs were also synthesized employing solutions of different AHM concentrations (0.01 M, 0.02 M and 0.05 M) to study the effect of the precursor concentration on the morphology, and the corresponding SEM images are shown in Fig. S6 (ESI†). The width of the hexagonal NRs synthesized at the AHM concentration of 0.01 M was the largest (700–800 nm) and their size decreased as the AHM concentration was increased to 0.02 (400–500 nm) and finally to 0.05 M
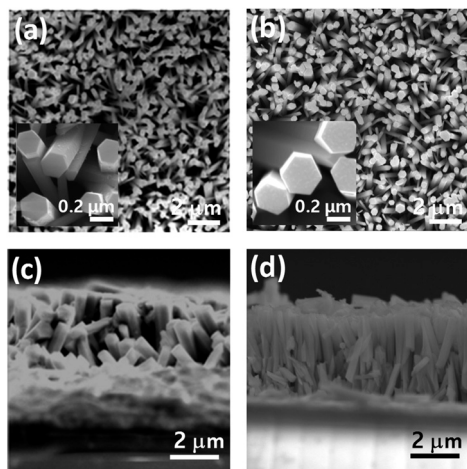
Fig. 2 Top and side views of vertically grown h-MoO₃ NRs on the FTO substrate at different irradiation times:, (a) and (c) 90 s and (b) and (d) 180 s, and zoom-in views (insets) with a MW power of 320 W in 0.02 M AHM.

Table 1 Average dimensions of vertically aligned h-MoO₃ NRs synthesized on FTO for various irradiation times at 320 W in 0.02 M AHM

Time (s)	Length (μm)	Diameter (μm)	Aspect ratio (μm)
90	2.75	0.26	10.6
180	3.75	0.31	12.01
300	5.84	0.42	13.9

(250–350 nm) (Table S1c, ESI†). Consequently, the density of NRs on the substrate followed a reverse trend, with the number of NRs per unit area being the highest for the highest precursor concentration. A higher concentration of the precursor solution results in the formation of more nucleation sites which in turn increases the number of NRs grown per unit area.[24]
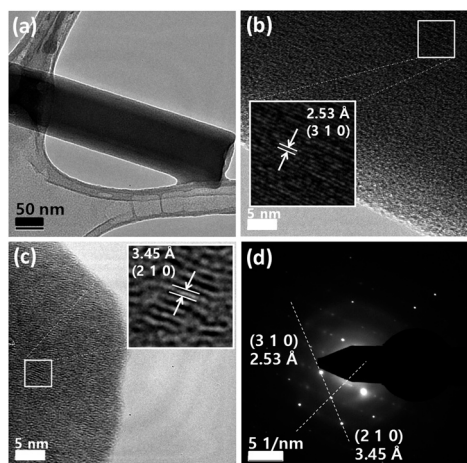
Fig. 3 (a) Low and (b) and (c) high resolution TEM images and their respective zoom-in views (insets); (d) SAED pattern of h-MoO₃ NRs obtained with 320 W power irradiation for 300 s in 0.02 M AHM on the FTO substrate.

Fig. 3 shows the transmission electron microscopy (TEM) images of the as-synthesized h-MoO₃ NRs. The hexagonal NRs with an approximate rod diameter of 200 nm can be clearly observed in the low resolution image (Fig. 3a). The high resolution-TEM images show well resolved lattice fringes with interplanar spacings corresponding to the (310) and (210) planes of h-MoO₃ (Fig. 3b and c). The electron diffraction pattern from the side facets of the nanorod in Fig. 3d matches very well with the lattice fringe analysis as well as the XRD measurements.

There are ample studies in the literature on the synthesis and growth mechanism of h-MoO₃ with AHM as the precursor.[12,13,25] The reaction proceeds by the dissociation of AHM in water to release ammonia (NH_4^+) and molybdate ions, $(Mo_7O_{24})^{6-}$. These $(Mo_7O_{24})^{6-}$ ions are then oxidised in the presence of concentrated nitric acid to precipitate MoO_3 crystals. The growth mechanism for the formation of vertically aligned h-MoO₃ nanostructures involves two steps: nucleation and growth. The seeding step involves the formation of tiny nuclei on the substrate which are high-energy sites from which the crystal propagation starts. The MoO_6 building blocks start to grow along the c-axis with assistance of NH_4^+ ions and along the a-axis with the help of OH^- ions, resulting in an anisotropic growth along the preferred orientation. This is followed by the growth of such crystallites, which results in the formation of larger hexagons.[14] To study the effect of NH_4^+ ions during the growth of the metastable h-MoO₃ crystals, we performed a control experiment in solution with an NH_4^+-free molybdenum precursor, $MoCl_5$, keeping the other reaction conditions the same. The synthesis resulted in the formation of a white powder consisting of only α-MoO_3, as characterized by SEM, XRD and Raman spectroscopy (Fig. S7, ESI†). This confirmed the important role of NH_4^+ ions in the formation of metastable h-MoO₃. It is well reported that in the preparation of metal oxide nanostructures, ions such as SO_4^{2-}, Cl^-, and NH_4^+ act as structure directing agents (SDAs). These ions adsorb on the seed or nuclei, thereby reducing the surface energy in that orientation, which subsequently stops the growth in that direction, allowing the seed to grow only in the available direction.[15,16,26,27] The h-MoO₃ phase is generally formulated as $(A_2O)_x \cdot MoO_3 \cdot (H_2O)_y$, where A = NH_4^+ or alkali metal ions. In the case of AHM, interactions with H_2O and NH_4^+ ions stabilize the metastable phase giving rise to h-MoO₃ NRs.[13,14]

To study the phase transformation of the metastable phase to the thermodynamically stable phase, the as-deposited vertically aligned h-MoO₃ thin films were slowly annealed (1° min⁻¹) at a temperature of 450 °C for 4 h in an air atmosphere. The slow annealing resulted in the phase and morphological transformation of the vertically aligned hexagonal-MoO₃ NRs to vertical α-MoO₃ NRs. The XRD pattern of the post annealed sample (Fig. 4a) shows diffraction peaks matching well with the standard reference for α-MoO_3 (JCPDS no. 05-0508) and Raman spectroscopy further confirmed that the post annealed samples belong to the stable alpha phase of MoO_3 (Fig. S7c†). From the SEM
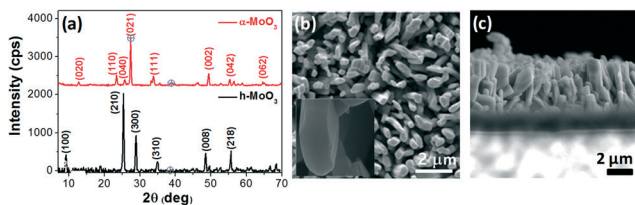
Fig. 4 (a) XRD pattern, (b) top view, zoom-in view (inset) and (c) cross sectional SEM images showing the effect of annealing on oriented h-MoO$_3$ NRs.
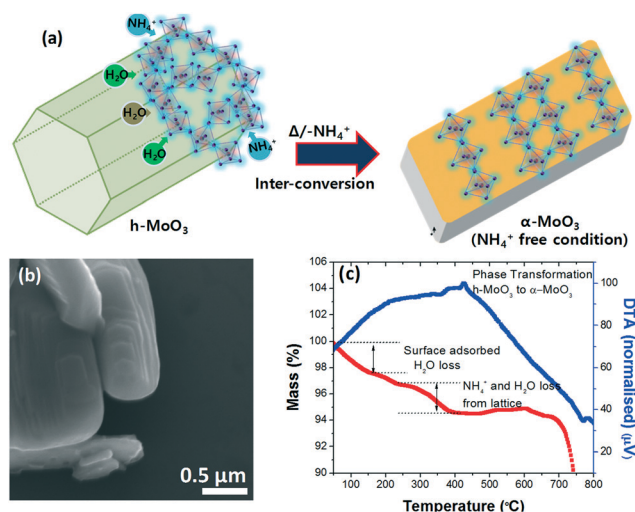

Fig. 5 (a) Schematic diagram, (b) FESEM analysis indicating a layered structure and (c) TG/DTA curves showing the effect of annealing on h-MoO$_3$ NRs.

images of the annealed sample (Fig. 4b), it is evident that the hexagonal crystallites have transformed into two-dimensional orthorhombic crystallites preserving the vertical alignment (Fig. 4c) of the rods with a layered structure, and a schematic of the same is given (Fig. 5a and b). This transformation is consistent with the loss of NH$_4^+$ ions in thermogravimetric analysis (TGA) and the corresponding exothermic peak is seen at ~400 °C in the differential thermal analysis (DTA) curves (Fig. 5c), indicating an irreversible phase transformation. The average length, width and breadth of the converted MoO$_3$ NRs were calculated to be 3.3, 0.75 and 0.34 μm, respectively.

The UV-visible absorbance spectra of the as-grown h-MoO$_3$ and annealed α-MoO$_3$ film are presented in Fig. S8a (ESI†). As can be seen, both h-MoO$_3$ and α-MoO$_3$ strongly absorb only in the UV region and are highly transparent in the visible region. The photoluminescence spectra of the h-MoO$_3$ and α-MoO$_3$ rods on FTO at room temperature (λ_{ex} = 320 nm) closely resemble each other (Fig. S8b, ESI†). The main emission peak is centered at 391 nm for h-MoO$_3$ NRs and at 393 nm for α-MoO$_3$ rods. The optical band gaps for h-MoO$_3$ and α-MoO$_3$ calculated from the corresponding diffuse reflec-

tance spectra using the Kubelka–Munk function are 2.86 and 3.21 eV, respectively (Fig. S8c, S8d and S9, ESI†).

In summary, vertically aligned metastable hexagonal MoO$_3$ NRs on different substrates have been synthesized employing MW irradiation within a short time of 90 s. The dimensions and density of the NRs can be tuned by appropriately varying the synthesis time, choice of substrate and precursor concentration. The optimized conditions for obtaining defect free vertically aligned h-MoO$_3$ NRs with dimensions of 5.8 μm length and 420 nm diameter are achieved at a MW irradiation power of 320 W for 300 s in 0.02 M AHM on seeded FTO. Further, the h-MoO$_3$ NRs have been completely transformed into α-MoO$_3$ NRs by annealing in air preserving the vertical alignment. This study paves the way for the controlled generation of MoO$_3$ NRs on different substrates in a short period of time with the potential to fabricate various electrochromic, photo-electrochemical and photovoltaic devices based on such well aligned vertical NRs.

Conflicts of interest

There are no conflicts to declare.

Acknowledgements

Notes and references

1 W. Stark, P. Stoessel, W. Wohlleben and A. Hafner, *Chem. Soc. Rev.*, 2015, **44**, 5793–5805.
2 T. Guo, M.-S. Yao, Y.-H. Lin and C.-W. Nan, *CrystEngComm*, 2015, **17**, 3551–3585.
3 B. Lebeau and P. Innocenzi, *Chem. Soc. Rev.*, 2011, **40**, 886–906.
4 K. H. Kim, K. M. Cho, D. W. Kim, S. J. Kim, J. Choi, S. J. Bae, S. Park and H.-T. Jung, *ACS Appl. Mater. Interfaces*, 2016, **8**, 5556–5562.
5 T. Alammar, I. I. Slowing, J. Anderegg and A.-V. Mudring, *ChemSusChem*, 2017, **10**, 3387–3401.
6 K. Polychronopoulou, A. F. Zedan, M. Katsiotis, M. Baker, A. AlKhoori, S. Y. AlQaradawi, S. Hinder and S. AlHassan, *Mol. Catal.*, 2017, **428**, 41–55.
7 R. Gedye, F. Smith, K. Westaway, H. Ali, L. Baldisera, L. Laberge and J. Rousell, *Tetrahedron Lett.*, 1986, **27**, 279–282.
8 R. J. Giguere, T. L. Bray, S. M. Duncan and G. Majetich, *Tetrahedron Lett.*, 1986, **27**, 4945–4948.
9 I. Bilecka and M. Niederberger, *Nanoscale*, 2010, **2**, 1358–1374.
10 Z. Chen, D. Cummins, B. N. Reinecke, E. Clark, M. K. Sunkara and T. F. Jaramillo, *Nano Lett.*, 2011, **11**, 4168–4175.

11 V. Ramakrishnan, H. Kim, J. Park and B. Yang, *RSC Adv.*, 2016, **6**, 9789–9795.

12 H. Hu, C. Deng, J. Xu, K. Zhang and M. Sun, *J. Exp. Nanosci.*, 2015, **10**, 1336–1346.

13 A. Chithambararaj, N. Rajeswari Yogamalar and A. C. Bose, *Cryst. Growth Des.*, 2016, **16**, 1984–1995.

14 A. Chithambararaj, N. Sanjini, A. C. Bose and S. Velmathi, *Catal. Sci. Technol.*, 2013, **3**, 1405–1414.

15 S. Rajagopal, M. Bharaneswari, D. Nataraj, O. Khyzhun and Y. Djaoued, *RSC Adv.*, 2016, **6**, 88287–88299.

16 S. Rajagopal, D. Nataraj, O. Y. Khyzhun, Y. Djaoued, J. Robichaud, K. Senthil and D. Mangalaraj, *CrystEngComm*, 2011, **13**, 2358–2368.

17 P. Ayyub, *J. Cluster Sci.*, 2009, **20**, 429–451.

18 I. Gonzalez-Valls and M. Lira-Cantu, *Energy Environ. Sci.*, 2009, **2**, 19–34.

19 A. Chithambararaj, N. Rameshbabu and A. C. Bose, *Sci. Adv. Mater.*, 2014, **6**, 1302–1312.

20 M. Osaka, K. Tanaka, S. Sekine, Y. Akutsu, T. Suzuki and H. Mimura, *J. Nucl. Mater.*, 2012, **427**, 384–388.

21 M. Santos-Beltrán, F. Paraguay-Delgado, R. García, W. Antúnez-Flores, C. Ornelas-Gutiérrez and A. Santos-Beltrán, *J. Mater. Sci.: Mater. Electron.*, 2017, **28**, 2935–2948.

22 W. Pan, R. Tian, H. Jin, Y. Guo, L. Zhang, X. Wu, L. Zhang, Z. Han, G. Liu and J. Li, *Chem. Mater.*, 2010, **22**, 6202–6208.

23 L. Zheng, Y. Xu, D. Jin and Y. Xie, *J. Mater. Chem.*, 2010, **20**, 7135–7143.

24 T. Ma, M. Guo, M. Zhang, Y. Zhang and X. Wang, *Nanotechnology*, 2007, **18**, 035605.

25 A. Dhara, G. Hodes and S. K. Sarkar, *RSC Adv.*, 2014, **4**, 53694–53700.

26 S. Rajagopal, D. Nataraj, D. Mangalaraj, Y. Djaoued, J. Robichaud and O. Y. Khyzhun, *Nanoscale Res. Lett.*, 2009, **4**, 1335.

27 S. Rajagopal, H.-M. Lee, K. Lee and C.-K. Kim, *Korean J. Chem. Eng.*, 2013, **30**, 1833–1835.